nature synthesis

Article

https://doi.org/10.1038/s44160-025-00951-z

Catalytic asymmetric activation of bicyclobutanes

Received: 18 June 2025

Accepted: 3 November 2025

Published online: 05 January 2026

Check for updates

Fuxing Shi[1], Nils Frank[1], Markus Leutzsch[1], Chendan Zhu[1], Nobuya Tsuji[2] & Benjamin List[1,2]

The precise manipulation of unfunctionalized hydrocarbons remains a fundamental challenge for chemical synthesis and catalysis. Stereodifferentiation in strained alkanes is particularly difficult to accomplish because a catalyst has to distinguish various highly exergonic chemo- and stereoselective strain-release channels. Here we disclose an organocatalytic asymmetric hydroalkoxylation of bicyclobutanes with alcohols to efficiently access tertiary cyclopropylcarbinyl ethers with high enantioselectivity (e.r. up to 98:2). Enantiocontrol is accomplished through chiral recognition between the confined iminoimidodiphosphoric acid catalyst and the substrate, mediated by non-covalent interactions between a Lewis basic binding site of the confined anion and the polarized C–H bond of the cyclopropylcarbinyl ion intermediate. Our work establishes bicyclobutane activation by harnessing strain-release energetics while maintaining precise stereo- and regiocontrol through structural confinement.

Although Baeyer introduced the 'ring strain' concept as long ago as 1885[1], strain-release chemistry has experienced a renaissance over the past decade as a transformative strategy for molecular manipulation[2]. Strain-release tactics are used to create versatile synthetic intermediates, finding broad applications across total synthesis[3], polymer science[4,5] and bio-orthogonal chemistry[6,7]. Representative examples include the radical/anionic ring opening of [1.1.1]propellane towards bicyclo[1.1.1]pentanes[8–11], structural analogues that serve as three-dimensional bioisosteres for planar *para*-substituted arenes due to their matching substituent vectors[12,13]. Parallel advances use [3.1.1]propellane to construct bicyclo[3.1.1]heptanes through radical-mediated pathways, establishing *meta*-arene bioisosterism (Fig. 1a)[14,15]. Despite these successes, the activation of simpler hydrocarbon-based bicyclo[1.1.0]butanes (BCBs) remains underexplored[16–18], presumably due to the intermediacy of cyclopropylcarbinyl and non-classical bicyclobutonium carbocations[19], the dynamic behaviour of which is difficult to control[20]. Functionalized BCB derivatives bearing ketone, ester or amine groups have been extensively investigated[21–23]. These functional groups often act as stabilizing and directing groups and enable diverse transformations, including cycloadditions, C–C couplings and radical processes[24–26]. In contrast, the absence of such coordinating functionalities in hydrocarbon BCBs fundamentally impedes selective bond activation and enantiocontrol and enhances side reactions (see below), complicating efforts to harness their strain energy.

Our research group has developed a class of chiral Brønsted acid catalysts, including imidodiphosphate (IDP), imidodiphosphorimidates (IDPis) and iminoimidodiphosphates (iIDPs)[27–30], which exhibit extraordinary acidity and spatial confinement effects. These catalysts have previously demonstrated remarkable efficacy in activating inert hydrocarbon systems through cyclopropane ring-opening reactions and controlling stereoselectivity in Wagner–Meerwein rearrangements[31–33].

Inspired by these investigations, we envisioned applying this catalytic platform to resolve the long-standing challenges in BCB hydrocarbon activation, in which the absence of directing groups has historically hindered both reactivity modulation and stereochemical control. We hypothesize that stereochemistry may be controlled through the stabilization of the cyclopropylcarbinyl–bicyclobutonium cation intermediate within the enzyme-like chiral environments of our IDP-type catalysts. In this study, we report the enantioselective hydroalkoxylation of BCB hydrocarbons using alcohols as nucleophiles, yielding enantioenriched ether products with up to 98:2 e.r. (Fig. 1b). The synthetic utility of these

[1]Max-Planck-Institut für Kohlenforschung, Mülheim an der Ruhr, Germany. [2]Institute for Chemical Reaction Design and Discovery (WPI-ICReDD), Hokkaido University, Sapporo, Japan. e-mail: list@kofo.mpg.de

https://doi.org/10.1038/s44160-025-00951-z

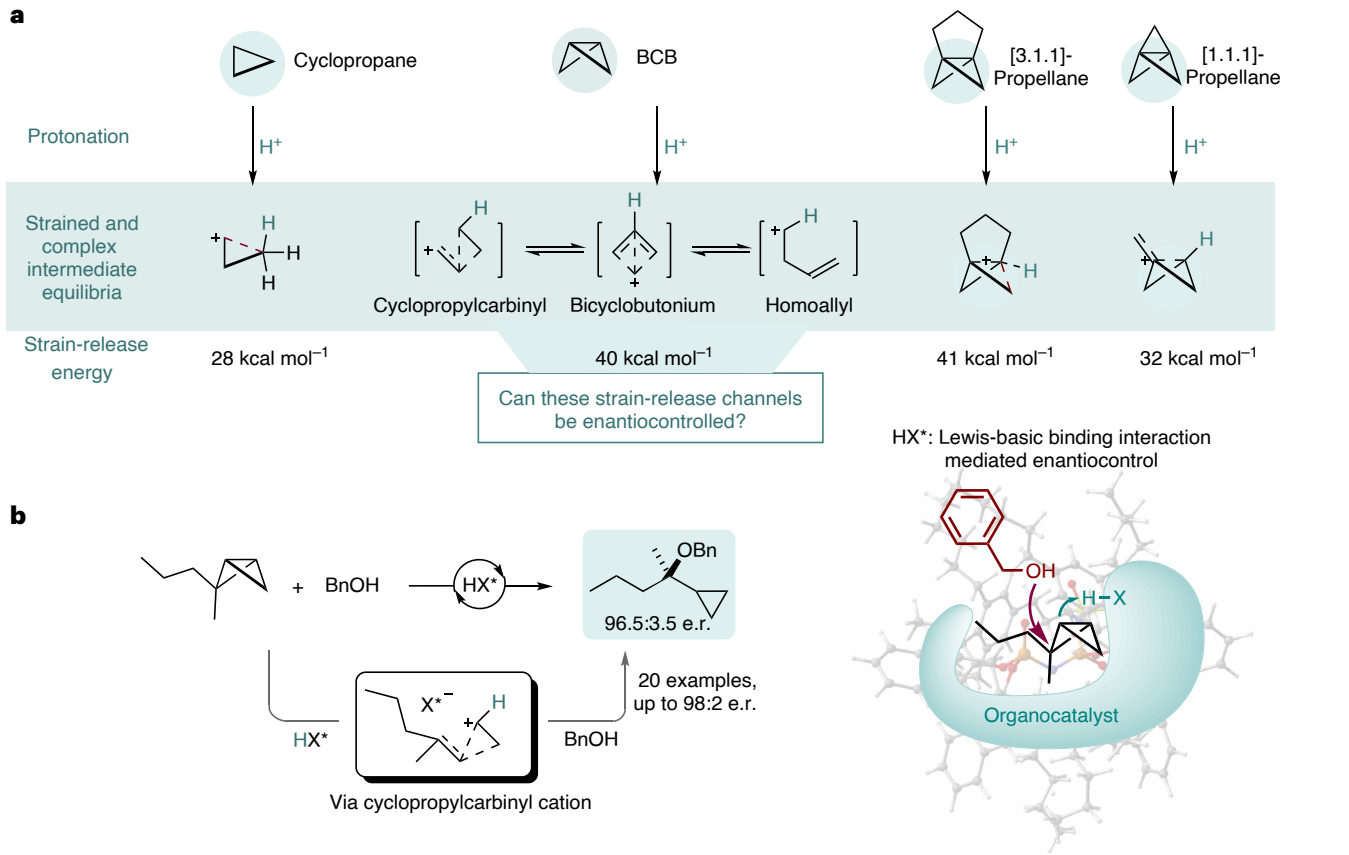

Fig. 1 | Progress in strain-release chemistry. a, Strain-release alkane activation and calculated strain-release energies for strained alkanes[8]. **b**, Our design: asymmetric organocatalytic hydrocarbon BCB activation. HX*, chiral Brønsted acid; Bn, benzyl.

ethers lies in their facile conversion to chiral tertiary alcohols—key intermediates in pharmaceuticals and materials science[34].

At the onset of our study, several organic chiral Brønsted acids were tested in the targeted ring-opening of substrate **1d**. The mild and unconfined chiral phosphoric acid (CPA) delivered the desired product **3d** with poor enantiocontrol and a high yield of side product **4**. However, our confined IDP catalyst **2a** gave product **3d** in moderate yield and a high e.r. of 93.5:6.5. We found that its sterically congested 2,4,6-tripentyl phenyl substitution was crucial in achieving excellent selectivity and enantiocontrol. Using the same 2,4,6-tripentyl phenyl substitution in the more acidic sulfonylimidophosphoryl iIDP catalyst sustained the high enantioselectivity (96.5:3.5 e.r.), while increasing the yield of **3a** and reducing the amount of unwanted 'cracking' side product **4**. Compared with the chemoselectivity of IDP **2a** and iIDP **2d**, stronger acids enhance alcohol trapping to give the ether, whereas weaker acids favour elimination. To visually assess this substituent effect, buried volumes were calculated using a model of the substrate in the catalyst pocket[35,36] (Fig. 2). A higher percentage of buried volume, which corresponds to a narrower pocket, may indicate that the substrate is stabilized within the iIDP pocket by non-covalent interactions, possibly compensating for the absence of traditional heteroatom or resonance stabilization.

Compared with iIDP **2b** (47.2% buried volume) and **2c** (58.8% buried volume), the tripentyl-substituted iIDP **2d** has a more confined microenvironment, leading to stronger enantiocontrol on the BCB substrate. Despite having good chemoselectivity, IDPi **2e** (74.3% buried volume) unexpectedly showed negligible enantiocontrol (53.5:46.5 e.r.). We hypothesized that the Lewis basic phospho-oxy moiety (P=O) of the iIDP **2d** had a crucial effect on the chiral recognition of the BCB substrate (see below). Collectively, a precise balance between Brønsted acidity, confinement and oxy Lewis basicity seems to be essential to achieve good chemoselectivity, enantiocontrol and overall reactivity.

After a further screening of catalysts and reaction conditions, we selected iIDP **2d**, *n*-heptane (0.1 M) at −40 °C for 3 h as the optimal reaction conditions to afford product **3d** in good yield and excellent enantioselectivity (71%, 96.5:3.5 e.r.).

With optimized conditions in hand, we investigated the substrate scope (Fig. 3). First, benzyl alcohol was used as the nucleophile: alkyl chain (−R^1)-substituted BCBs gave products **3a**–**3d** in good yields and excellent enantioselectivities (61–75%, 96.5:3.5–98:2 e.r.), albeit moderate enantioselectivity was obtained with an ethyl group (**3e**, 84.5:15.5 e.r.). Unfortunately, low yields of **3f** and **3g**—containing branched alkyl substituents on −R^1—were displayed with **3g** exceptionally displaying high enantioselectivity (**3g**, 93.5:6.5 e.r.). A substrate bearing a chloroalkyl substituent was well tolerated, providing product **3h** with an e.r. of 95.5:4.5 in 65% yield. The aryl-substituted alkyl chain substrate reacts efficiently with benzyl alcohol, affording products **3i** and **3j** in good yield with excellent enantioselectivity. Subsequently, we examined various alcohol nucleophiles with two representative BCB substrates (**1c** and **1d**): *n*-butanol as the nucleophile gave products **3k** and **3o** in good yields and excellent enantioselectivities. To our delight, the smallest alcohol, methanol, displayed excellent yield and equally high enantioselectivity for product **3l** (67% yield, 93.5:6.5 e.r.). Further, allylic alcohols (**3m** and **3n**), 2-methoxyethan-1-ol (**3r**) and phenylethanol (**3q**) added to BCBs resulted in good yields and excellent enantioselectivities. Branched nucleophiles, such as isopropanol, resulted in low product yields, but excellent enantioselectivities were retained (**3p**, 96:4 e.r.). The reaction could be applied to the natural monoterpenoids *R*-(+)-citronellol and *S*-(−)-citronellol, leading to products **3s** and **3t**, respectively, in good yields and excellent catalyst-controlled diastereoselectivity. The tertiary alcohol products **5d** and **5i** could be prepared from the benzyl ether precursors **3d** and **3i** in excellent yields, without erosion of enantiopurity under simple hydrogenation

https://doi.org/10.1038/s44160-025-00951-z

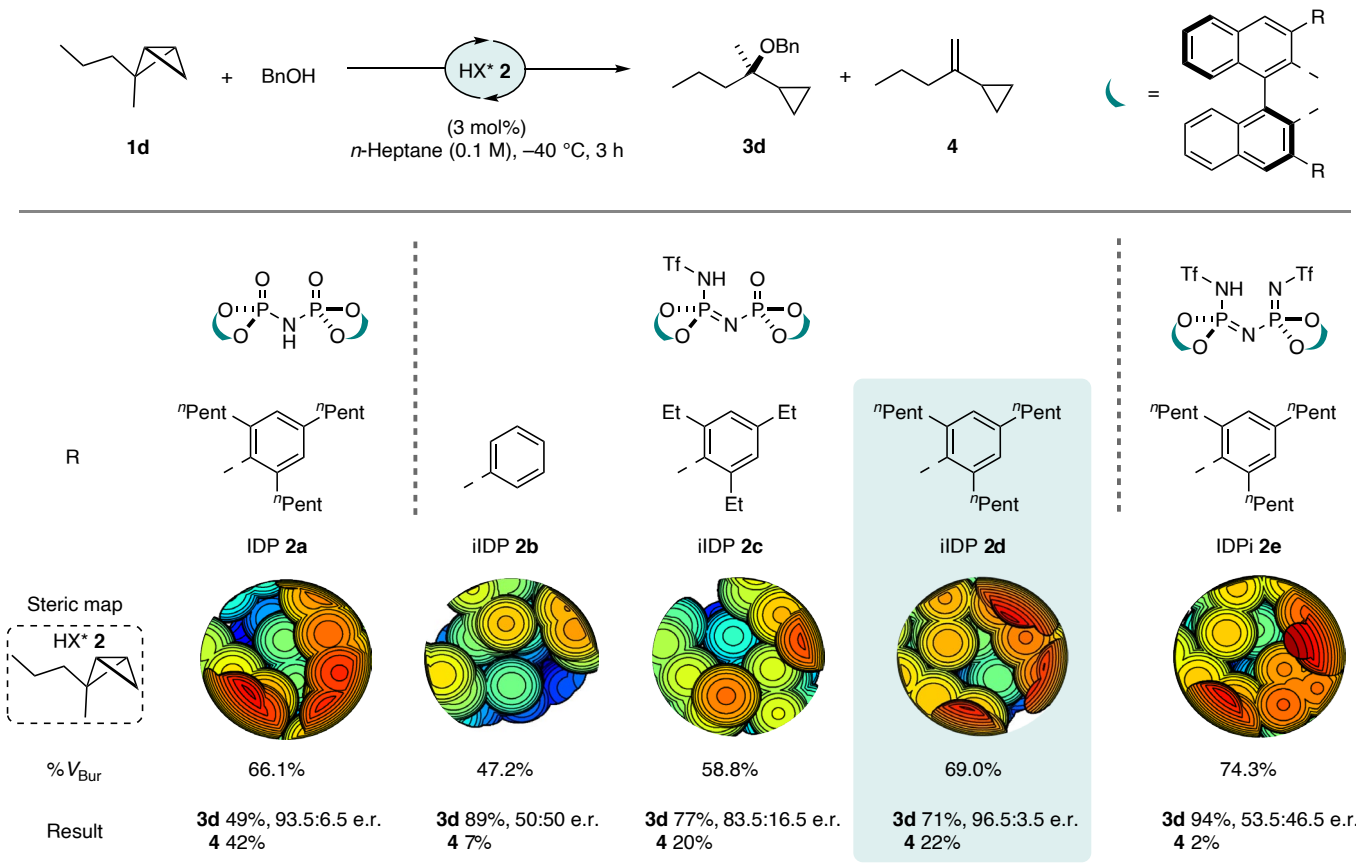

Fig. 2 | Investigation of acidity, confinement and chiral pocket size of the catalyst in the catalytic BCB activation. Yields were determined by ^{1}H NMR spectroscopy using CH_2Br_2 as the internal standard. The e.r. was determined by gas chromatography analysis (see Supplementary Section 9 for further details). Calculated steric map of simplified substrate visualized by SambVca 2.1[46]. The map is viewed from the centre of the substrate and directed toward the active site of each catalyst. The colour indicates the depth along the *z* axis; the red zone is closer to the substrate, whereas the blue zone is farther away. BnOH, benzyl alcohol; ^{n}Pent, *n*-pentyl; Et, ethyl; $\%V_{Bur}$, buried volume.

conditions (10 mol% Pd/C, H_2). X-ray diffraction analysis of ester **8**, derived from the tertiary alcohol **5i**, allowed the unambiguous determination of the absolute configurations of the obtained products to be (*R*)-configured[37,38].

Mechanistically, we speculated that the reaction proceeds via a stepwise protonation of BCB **1c** to form the corresponding carbocation, which is subsequently attacked by the alcohol nucleophile. However, a concerted mechanism in which protonation and C–O bond formation occur simultaneously is also plausible[39,40]. To explore the mechanism, we conducted a series of experimental and theoretical investigations. We found that the reaction of deuterated benzyl alcohol with BCB **1d** afforded the corresponding deuterated benzyl ether **3d²** with 85% deuterium incorporation and **3d³** with 15% deuterium incorporation (Fig. 4a). This suggests that the protonation occurs from only one site, and the catalyst shows some site preference in the protonation. Kinetic profiling by ^{1}H NMR spectroscopy shows that hydroalkoxylation and decomposition of BCB **1c** are parallel and not consecutive processes (Fig. 4b). In addition, we performed a control experiment using isolated **4** and BnOH as the starting material under the standard reaction conditions, and no reactivity was observed. Overall, the olefin by-product is inactive towards hydroalkoxylation, excluding it as a productive intermediate in the reaction mechanism.

Notably, Olah et al. reported in 1992 that cyclopropylcarbinyl intermediates could arise from cyclopropanol substrates[41]. Nevertheless, using cyclopropanes **6** or **7** with excess BnOH (5 equiv.) afforded product **3c** in poor enantioselectivity (Fig. 4c), in sharp contrast to the high selectivity observed from substrate **1c**. This rules out a cyclopropylcarbinyl pathway under our conditions and further sets our system mechanistically apart from Patel and Marek's stereospecific generation of such cations from chiral homoallylic alcohols[42]. To investigate the mechanism, density functional theory studies were performed at the CPCM(heptane)-PBE0-D3(BJ)/def2-TZVP//CPCM(heptane)-PBE0-D3(BJ)/def2-SVP level of theory (Fig. 4d; see Supplementary Section 11 for further details)[43–45]. The iIDP/BnOH complex **B** is more stable ($\Delta G^{\ddagger}$ = −13.8 kcal mol^{-1}) than the iIDP/**1d** complex **C** ($\Delta G^{\ddagger}$ = −9.7 kcal mol^{-1}), suggesting that the more basic BnOH binds more strongly to the iIDP pocket than the substrate **1d**. The Gibbs free activation energy from **B** to (***R***)-**TS2** ($\Delta G^{\ddagger}$ = 2.2 kcal mol^{-1}) supports a concerted, although asynchronous mechanism, in which the reaction is triggered by the protonation of the BCB followed by C–O bond formation. The transition state conformer (***R***)-**TS2** leading to the (***R***)-**3d** is 2.4 kcal mol^{-1} lower compared with the conformer (***S***)-**TS2** leading to (***S***)-**3d**. This is in reasonable agreement with the experimental e.r. of 96.5:3.5.

To further understand why iIDP **2d** leads to superior enantioselectivities, while IDPi **2e** results in poor enantioselectivities, non-covalent interaction plots were generated (Fig. 4e). The transition states (***R***)-**TS3** and (***S***)-**TS3** for IDPi catalysis display only non-directional dispersion interactions (N^1–H^2 distance, 2.45 Å for (***R***)-**TS3** and 2.49 Å for (***S***)-**TS3**) with the substrate. In stark contrast, in iIDP catalysis (***S***)-**TS2** exhibits a well-defined, spatially oriented hydrogen bonding between the Lewis-basic component (P=O) of the iIDP fragment and the polarized C–H bond at the methyl group of the cyclopropylcarbinyl cation. Moreover, in the favoured (***R***)-**TS2**, another hydrogen bond between iIDP and the protonated hydrogen of the cyclopropyl moiety is also present, whereas this interaction is absent in (***S***)-**TS2**. This leads to

https://doi.org/10.1038/s44160-025-00951-z

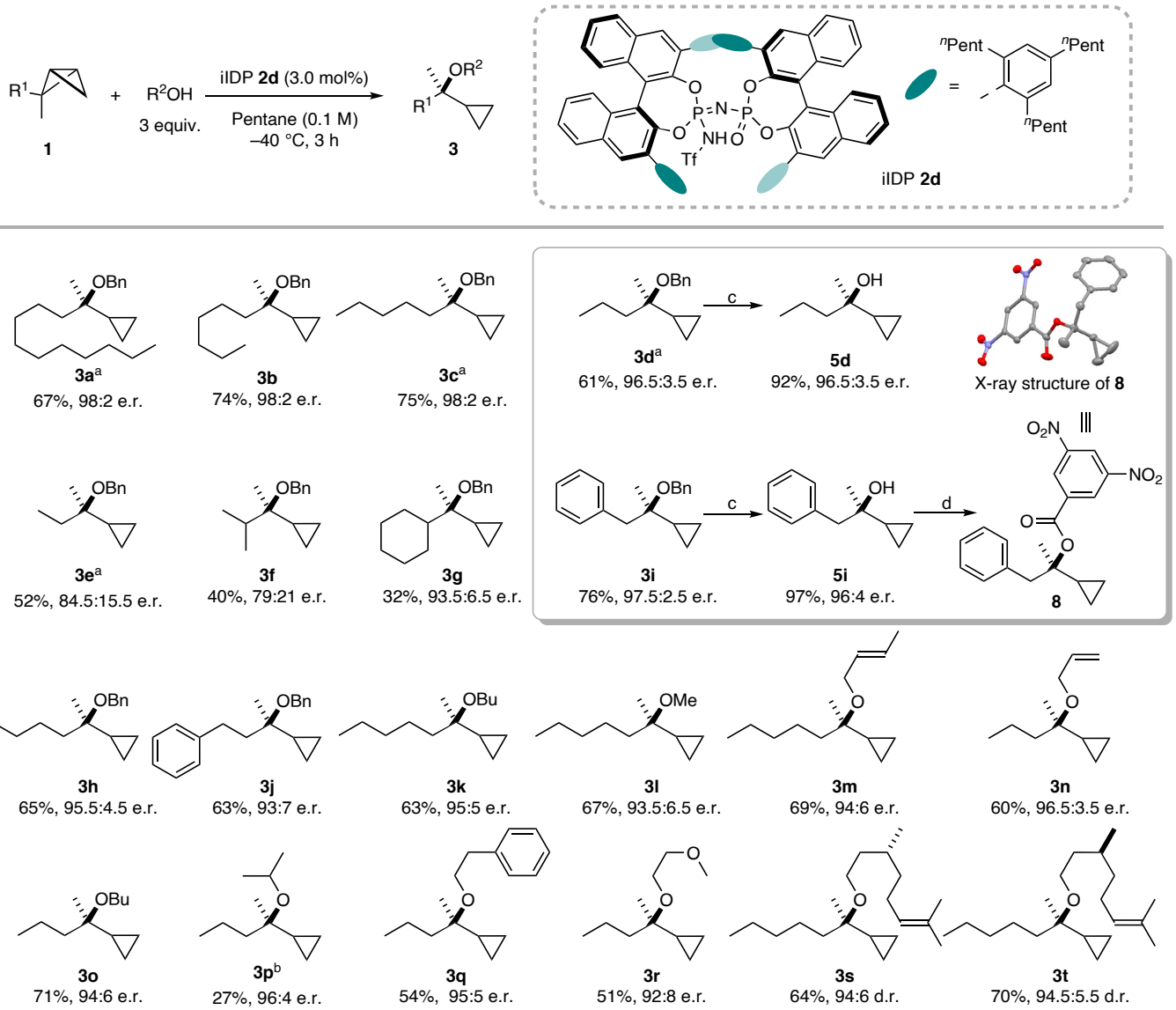

Fig. 3 | Scope of the catalytic asymmetric BCB activation. Reactions were performed at 0.1-mmol scale. Isolated yields after chromatographic purification. The e.r. was determined by gas chromatography and high-performance liquid chromatography analysis (see Supplementary Section 9 for further details). Atom colour coding of X-ray structure **8**: C, grey; O, red; N, blue. [a]With 3 equiv. ROH in heptane (0.1 M) for 3 h. [b]With 4 mol% catalyst and 4 equiv. BnOH. [c]With 10 wt% Pd/C and H_2 gas in methanol (0.1 M) for 12 h. [d]With 2 equiv. 3,5-dinitrobenzoyl chloride, 15% mol 4-dimethylaminopyridine and 6 equiv. triethylamine at room temperature for 12 h. Bu, butyl; Me, methyl.

preferred stabilization of (***R***)-**TS2** compared with (***S***)-**TS2**, in which these hydrogen bonds are less pronounced (O^1–H^1 distance, 2.08 Å; O^1–H^2 distance, 2.52 Å for (***R***)-**TS2**; O^1–H^1 distance, 2.21 Å for (***S***)-**TS2**), explaining the observed enantioselectivity.

A delicate interplay between Brønsted acidity, Lewis basicity and steric confinement of the iIDP catalyst class enables the asymmetric hydroalkoxylation of BCB alkanes using simple alcohols in enantioselectivities up to 98:2. Traditional directing groups and metal catalysts are not required and we demonstrate how molecular strain and confined catalyst design synergistically enable enantiocontrol in the strain release of hydrocarbon ring systems.

Methods

General procedure for the catalytic asymmetric BCB activation

A 5-ml vial was charged with IDPi **2d** (3.0 µmol, 3 mol%) and a magnetic stir bar under an atmosphere of argon. Dry pentane/heptane (1 ml) and alcohol (0.3 mmol, 3.0 equiv.) were added. The vial was cooled to −40 °C. The BCB substrate (0.1 mmol, 1.0 equiv.) was added dropwise at −40 °C and the reaction was stirred at −40 °C for 3 h. Afterwards, the reaction mixture was treated with triethylamine (0.1 mmol, 1 equiv.) at −40 °C. After the mixture had been stirred for 0.5 h, the solvent of the reaction mixture was directly removed under reduced pressure. The product was then collected by column chromatography on silica (methyl *tert*-butyl ether:cyclohexane = 1:30), and its e.r. determined by chiral high-performance liquid chromatography and gas chromatography.

Data availability

The experimental procedures and analytical data supporting the findings of the study are available in the paper and Supplementary Information. Crystallographic data for compound **8** are provided in Supplementary Information and are available free of charge from the Cambridge Crystallographic Data Centre (CCDC) under the deposition number CCDC 2451420.

https://doi.org/10.1038/s44160-025-00951-z

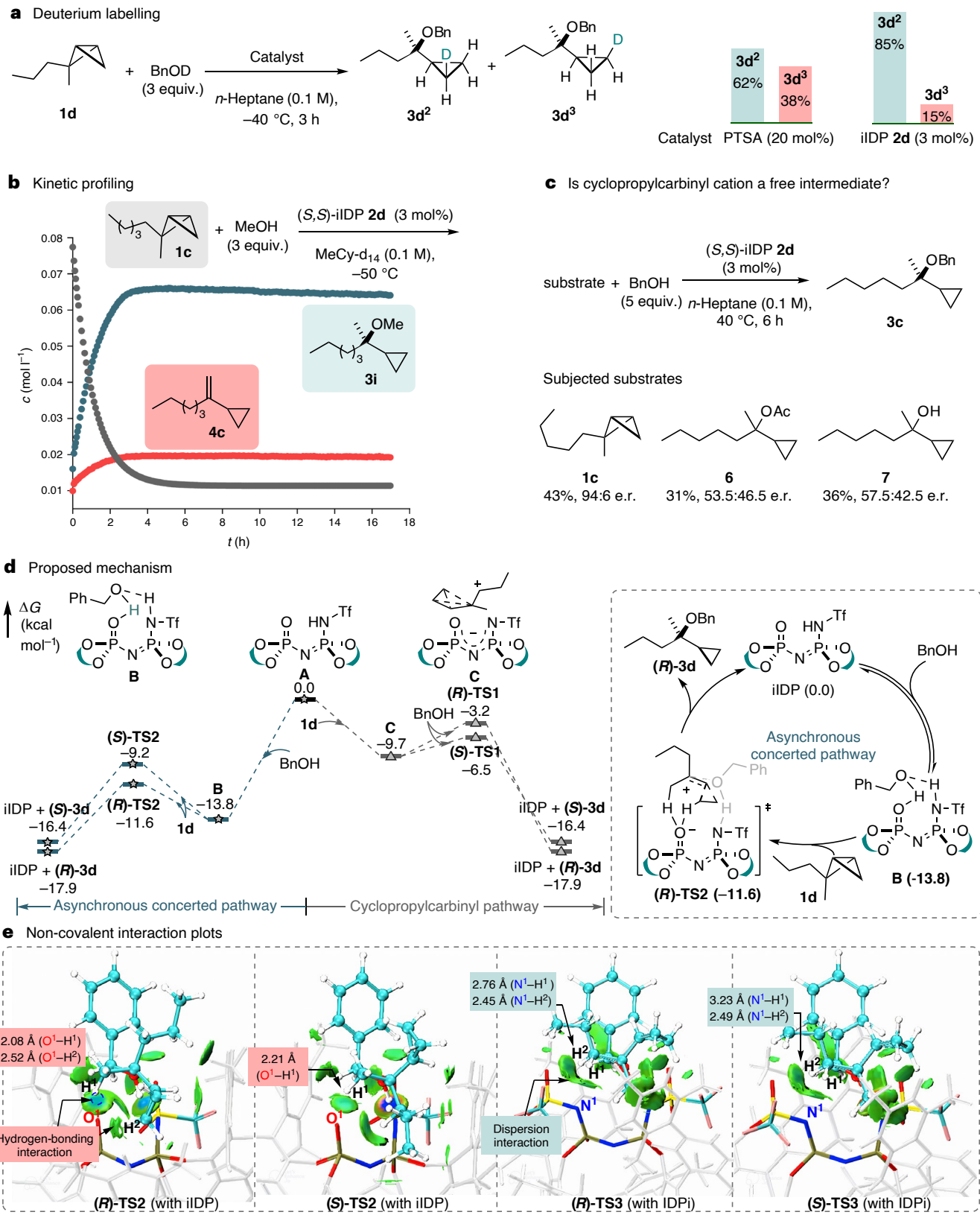

Fig. 4 | Mechanistic studies. a, Reaction of BCB **1c** with butanol-d_1. **b**, Reaction profile monitored by ^{1}H NMR spectroscopy, using **1d** as a substrate and methanol as a nucleophile. **c**, Hydroalkoxylation with BCB **1c** and etherification of the corresponding alcohol and ester. **d**, A plausible catalytic cycle and density functional theory study of the reaction mechanism. **e**, Comparison of the IGMH map between (*R*)-**TS2**, (*S*)-**TS2**, (*R*)-**TS3** and (*S*)-**TS3**. A green isosurface represents the dispersion interactions; a blue isosurface represents the hydrogen-bond interactions. PTSA, *p*-toluenesulfonic acid; MeCy, methylcyclohexane; TS, transition state.

References

1. Baeyer, A. Ueber polyacetylenverbindungen. *Berichte Dtsch. Chem. Ges.* **18**, 2269–2281 (1885).
2. Turkowska, J., Durka, J. & Gryko, D. Strain release—an old tool for new transformations. *Chem. Commun.* **56**, 5718–5734 (2020).
3. Ebner, C. & Carreira, E. M. Cyclopropanation strategies in recent total syntheses. *Chem. Rev.* **117**, 11651–11679 (2017).
4. Herzberger, J. et al. Polymerization of ethylene oxide, propylene oxide, and other alkylene oxides: synthesis, novel polymer architectures, and bioconjugation. *Chem. Rev.* **116**, 2170–2243 (2016).
5. Sathe, D. et al. Olefin metathesis-based chemically recyclable polymers enabled by fused-ring monomers. *Nat. Chem.* **13**, 743–750 (2021).
6. Agard, N. J., Prescher, J. A. & Bertozzi, C. R. A strain-promoted [3+2] azide–alkyne cycloaddition for covalent modification of biomolecules in living systems. *J. Am. Chem. Soc.* **126**, 15046–15047 (2004).
7. Tokunaga, K. et al. Bicyclobutane carboxylic amide as a cysteine-directed strained electrophile for selective targeting of proteins. *J. Am. Chem. Soc.* **142**, 18522–18531 (2020).
8. Sterling, A. J., Smith, R. C., Anderson, E. A. & Duarte, F. Beyond strain release: delocalization-enabled organic reactivity. *J. Org. Chem.* **89**, 9979–9989 (2024).
9. Wiberg, K. B. & Waddell, S. T. Reactions of [1.1.1]propellane. *J. Am. Chem. Soc.* **112**, 2194–2216 (1990).
10. Feller, D. & Davidson, E. R. Ab initio studies of [1.1.1]- and [2.2.2] propellane. *J. Am. Chem. Soc.* **109**, 4133–4139 (1987).
11. Wiberg, K. B. & Walker, F. H. [1.1.1]Propellane. *J. Am. Chem. Soc.* **104**, 5239–5240 (1982).
12. Gianatassio, R. et al. Strain-release amination. *Science* **351**, 241–246 (2016).
13. Lopchuk, J. M. et al. Strain-release heteroatom functionalization: development, scope, and stereospecificity. *J. Am. Chem. Soc.* **139**, 3209–3226 (2017).
14. Gassman, P. G. & Proehl, G. S. [3.1.1]Propellane. *J. Am. Chem. Soc.* **102**, 6862–6863 (1980).
15. Frank, N. et al. Synthesis of meta-substituted arene bioisosteres from [3.1.1]propellane. *Nature* **611**, 721–726 (2022).
16. Suresh, R., Orbach, N. & Marek, I. Synthesis of stereodefined polysubstituted bicyclo[1.1.0]butanes. *J. Am. Chem. Soc.* **146**, 13748–13753 (2024).
17. Thai-Savard, L. & Charette, A. B. Synthesis of 2-substituted bicyclo[1.1.0]butanes via zincocyclopropanation using bromoform as the carbenoid precursor. *Chem. Commun.* **59**, 5273–5276 (2023).
18. Li, Q.-H. et al. Nature-inspired catalytic asymmetric rearrangement of cyclopropylcarbinyl cation. *Sci. Adv.* **9**, eadg1237 (2023).
19. Olah, G. A., Surya Prakash, G. K. & Rasul, G. Ab initio/GIAO-CCSD(T) study of structures, energies, and ^{13}C NMR chemical shifts of $C_4H_7^+$ and $C_5H_9^+$ ions: relative stability and dynamic aspects of the cyclopropylcarbinyl vs bicyclobutonium ions. *J. Am. Chem. Soc.* **130**, 9168–9172 (2008).
20. McNamee, R. E., Frank, N., Christensen, K. E., Duarte, F. & Anderson, E. A. Taming nonclassical carbocations to control small ring reactivity. *Sci. Adv.* **10**, eadj9695 (2024).
21. Schwartz, B. D., Zhang, M. Y., Attard, R. H., Gardiner, M. G. & Malins, L. R. Structurally diverse acyl bicyclobutanes: valuable strained electrophiles. *Chem. Eur. J.* **26**, 2808–2812 (2020).
22. Hu, S., Pan, Y., Ni, D. & Deng, L. Facile access to bicyclo[2.1.1] hexanes by Lewis acid-catalyzed formal cycloaddition between silyl enol ethers and bicyclo[1.1.0]butanes. *Nat. Commun.* **15**, 6128 (2024).
23. Lin, S. L., Chen, Y. H., Liu, H. H., Xiang, S. H. & Tan, B. Enantioselective synthesis of chiral cyclobutenes enabled by Brønsted acid-catalyzed isomerization of BCBs. *J. Am. Chem. Soc.* **145**, 21152–21158 (2023).
24. Tyler, J. L. et al. Bicyclo[1.1.0]butyl radical cations: synthesis and application to [2π+2σ] cycloaddition reactions. *J. Am. Chem. Soc.* **146**, 16237–16247 (2024).
25. Tena Meza, A. et al. Sigma-bond insertion reactions of two strained diradicaloids. *Nature* **640**, 683–690 (2025).
26. Qin, T., He, M. & Zi, W. Palladium-catalysed [2σ+2π] cycloaddition reactions of bicyclo[1.1.0]butanes with aldehydes. *Nat. Synth.* **4**, 124–133 (2024).
27. Schreyer, L., Properzi, R. & List, B. IDPi catalysis. *Angew. Chem. Int. Ed.* **58**, 12761–12777 (2019).
28. Kaib, P. S., Schreyer, L., Lee, S., Properzi, R. & List, B. Extremely active organocatalysts enable a highly enantioselective addition of allyltrimethylsilane to aldehydes. *Angew. Chem. Int. Ed.* **55**, 13200–13203 (2016).
29. Schwengers, S. A. et al. Unified approach to imidodiphosphate-type Brønsted acids with tunable confinement and acidity. *J. Am. Chem. Soc.* **143**, 14835–14844 (2021).
30. Cheng, J. K., Xiang, S. H. & Tan, B. Imidodiphosphorimidates (IDPis): catalyst motifs with unprecedented reactivity and selectivity. *Chin. J. Chem.* **41**, 685–694 (2023).
31. Properzi, R. et al. Catalytic enantiocontrol over a non-classical carbocation. *Nat. Chem.* **12**, 1174–1179 (2020).
32. Raut, R. K. et al. Catalytic asymmetric fragmentation of cyclopropanes. *Science* **386**, 225–230 (2024).
33. Wakchaure, V. N. et al. Catalytic asymmetric cationic shifts of aliphatic hydrocarbons. *Nature* **625**, 287–292 (2024).
34. Stymiest, J. L., Bagutski, V., French, R. M. & Aggarwal, V. K. Enantiodivergent conversion of chiral secondary alcohols into tertiary alcohols. *Nature* **456**, 778–782 (2008).
35. Poater, A. et al. Thermodynamics of N-heterocyclic carbene dimerization: the balance of sterics and electronics. *Organometallics.* **27**, 2679–2681 (2008).
36. Poater, A., Ragone, F., Mariz, R., Dorta, R. & Cavallo, L. Comparing the enantioselective power of steric and electrostatic effects in transition-metal-catalyzed asymmetric synthesis. *Chem. Eur. J.* **16**, 14348–14353 (2010).
37. Zhang, M. et al. Stereocontrolled pericyclic and radical cycloaddition reactions of readily accessible chiral alkenyl diazaborolidines. *Angew. Chem. Int. Ed.* **61**, e202205454 (2022).
38. Liu, J., Cao, W. & You, S. Ligand-enabled *Z*-retentive Tsuji–Trost reaction. *Chem.* **10**, 1295–1305 (2024).
39. Khomutnyk, Y. Y. et al. Studies of the mechanism and origins of enantioselectivity for the chiral phosphoric acid-catalyzed stereoselective spiroketalization reactions. *J. Am. Chem. Soc.* **138**, 444–456 (2016).
40. Tsuji, N. et al. Activation of olefins via asymmetric Brønsted acid catalysis. *Science* **359**, 1501–1505 (2018).
41. Olah, G. A., Prakash Reddy, V. & Surya Prakash, G. K. Long-lived cyclopropylcarbinyl cations. *Chem. Rev.* **92**, 69–95 (1992).
42. Patel, K. & Marek, I. Stereospecific molecular rearrangement via nucleophilic substitution at quaternary stereocentres in acyclic systems. *Nat. Chem.* **17**, 933–940 (2025).
43. Neese, F. The ORCA program system. *Wiley Interdiscip. Rev. Comput. Mol. Sci.* **2**, 73–78 (2012).
44. Lu, T. A comprehensive electron wavefunction analysis toolbox for chemists, Multiwfn. *J. Chem. Phys.* **161**, 082503 (2024).

45. Yepes, D., Neese, F., List, B. & Bistoni, G. Unveiling the delicate balance of steric and dispersion interactions in organocatalysis using high-level computational methods. *J. Am. Chem. Soc.* **142**, 3613–3625 (2020).
46. Falivene, L. et al. Towards the online computer-aided design of catalytic pockets. *Nat. Chem.* **11**, 872–879 (2019).

Acknowledgements

Generous support from the Max Planck Society, the Deutsche Forschungsgemeinschaft (DFG, German Research Foundation), a Leibniz Award to B.L., Germany's Excellence Strategy–EXC 2033–390677874–RESOLV, and the European Research Council (Early Stage Organocatalysis (ESO)) to B.L. Deepseek was used for language refinement for the initial manuscript; all content was author-reviewed and approved.

Author contributions

B.L. designed and oversaw the project. F.S. developed and optimized the BCB activation reaction. F.S., N.F. and N.T. performed the computational studies. M.L. designed and performed the NMR spectroscopy mechanistic studies. F.S. and C.Z. conducted the single-crystal investigation. F.S., N.F. and B.L. wrote the paper with contributions from all authors.

Funding

Open access funding provided by Max Planck Society.

Competing interests

B.L. is listed as an inventor on patent number WO 2017/037141 filed by the Max-Planck-Institut für Kohlenforschung covering the iIDP and IDPi catalyst class and its applications in asymmetric synthesis. Furthermore, B.L. is listed as an inventor on a patent on an improved synthesis of imidodiphosphoryl-derived catalysts using hexachlorophosphazonium salts (patent number EP 3 981 775 A1) filed by the Max-Planck-Institut für Kohlenforschung. F.S., N.F., C.Z., M.L. and N.T. declare no competing interests.

Additional information

Supplementary information The online version contains supplementary material available at https://doi.org/10.1038/s44160-025-00951-z.

Correspondence and requests for materials should be addressed to Benjamin List.

Peer review information *Nature Synthesis* thanks the anonymous reviewers for their contribution to the peer review of this work. Primary Handling Editor: Joel Cejas-Sánchez, in collaboration with the *Nature Synthesis* team.